Available online at www.elixirpublishers.com (Elixir International Journal)

Electrical Engineering

Elixir Elec. Engg . 154 (2021) 55345-55350

ISSN: 2229-712X

Change Detection in Synthetic Aperture Radar (SAR) Images

Shantha Selvakumari R, Ramya R and Ramya PS
Department of ECE, Mepco Schlenk Engineering College, Sivakasi, India.

ARTICLE INFO

Article history:
Received: 20 April 2021;
Received in revised form:
10 May 2021;
Accepted: 19 May 2021;

Keywords
Novel Fuzzy Local Information C Means Clustering,
Log and Mean Ratio Operator,
Image Fusion.

ABSTRACT

This paper presents change detection approach for synthetic aperture radar images based on log and mean ratio operators, image fusion and a novel fuzzy local information c means Clustering algorithm. The two multi-temporal SAR images are subjected to ratio operators. The log ratio operator is used to produce the difference image with enhanced low intensity pixels. The mean ratio operator suppresses the unchanged region and improves the homogeneity of the changed region. The difference image is then subjected to image fusion. To improve the intensity of the background pixels Wavelet based image fusion technique is used. The fused image is then subjected to a novel fuzzy algorithm which is Reformulated Fuzzy Local Information C Means Clustering Algorithm. Finally the total number of pixels varied from the difference image is calculated. The kappa and Percentage of correct classification values are more than other algorithms.

I. Introduction

Image change detection analyses the images of same place taken at different time interval to identify the changes acquired. Change detection in Satellite images have more difficulties compared to other images due to the presence of speckle noise. This paper has developed a change detection technique that uses a Reformulated Fuzzy Local Information C-Mean Clustering algorithm. This is used to find the Changed region in the two multi-temporal SAR images during the course of time. Satellite images are routinely applied for change detection to find out the area change in the earth's surface. In recent years SAR images have gained much importance because they are not affected by any environmental conditions such as rain, smoke, haze, sunlight, etc. So this provides valuable data for flood detection, forest cover change detection, sea ice change detection, land change detection, etc.As mentioned in the literature the change detection involves three steps 1) Pre-processing of the images 2) Producing the difference image by fusing log and mean ratio images 3) changed image analysis. The task of the first step is to reduce the noise this is done using the median filter. In the second step the images are compared pixel by pixel to find the changed region. The changed image is analysed using various algorithms and operators to check for the accuracy of the image. Finally the pixel variations are calculated by comparing the obtained difference image with the ground truth. The performance of the SAR image is mainly based on the difference image quality and the classification accuracy. To support these two performances we work through an unsupervised change detection technique .This technique is unique in the following two aspects 1) Finding the difference image by fusion of log and mean ratio operators. SAR images can be subjected either to subtraction operator or ratio operators to determine the changed region. Here we have used ratio operators since it is more robust than difference operator 2) a novel FLICM technique is used which is RFLICM (Reformulated Fuzzy Local Information C Means Clustering)], which is less sensitive to noise and to determine the changed region with distribution free assumptions.

II. Change detection techniques

The Flow chart of the proposed Change detection technique is shown in Fig a. The two SAR images are treated using median filter for noise removal, since the SAR image suffers mainly due to speckle noise. The next step of the process involves giving the two multi-temporal SAR images to a log and mean ratio operators separately. The difference image is then fused using wavelet fusion. In order to get more accurate classification the fused image is once again given to the median filter all the median filters used here are of same size. This technique enhances the intensity of the background pixels. In order to improve the accuracy of the changed region the proposed system (RFLICM) is used. Finally, the pixel variation is calculated.

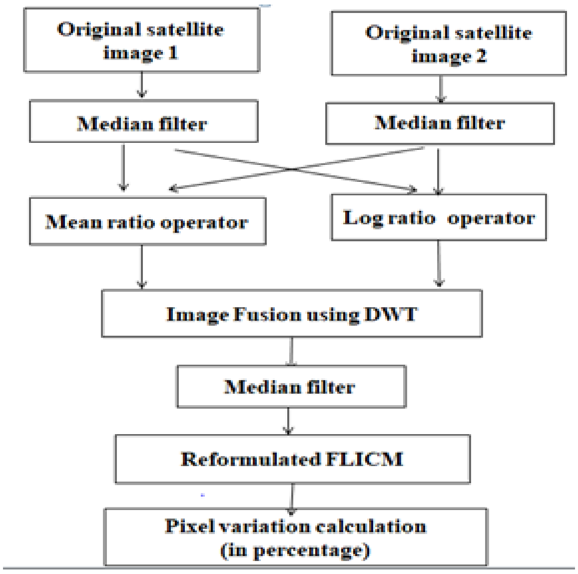

Fig 1. Flow chart of proposed change detection technique

A. Log And Mean Ratio Operators

As mentioned in section I for SAR images we use logarithmic or mean ratio operators. This is because of the presence of speckle noise and these two operators are more robust than the difference operators. In the past few years logarithmic operators are more concerned for SAR images because of its probability distribution for amplitude and intensity of SAR images. With the log operator the multiplicative speckle noise can be converted to additive noise components. Log operator produces difference image with enhanced low intensity pixels so the symmetry of the changed and unchanged regions can be made. But this operator does not detect changed region in the maximum extent since it weakens the high intensity pixel areas thus the mean ratio operator is used. The Mean Ratio operator is also more robust to the speckle noise and it produces the difference image by improving the homogeneity of the changed region. In an optimal difference image the changed areas exhibit larger values and unchanged exhibits more smaller value. The difference image should restore the background i.e. the unchanged area and should enhance the difference area information i.e. the changed area. Thus from the above analysis it is clear that the difference image obtained by the fusion of log and mean ratio operators provides more information than the individual difference image (i.e. Log and mean ratio operators).

The log ratio operator and mean ratio operator images are commonly given by

$$\mathbf{X_i} = \left|\mathbf{log_{10}}\left(\frac{\mathbf{X_2}}{\mathbf{X_1}}\right)\right| \tag{1}$$

$$\mathbf{X_m} = \mathbf{1} - \mathbf{min}\left(\frac{\mu_1}{\mu_2}, \frac{\mu_2}{\mu_1}\right) \tag{2}$$

X_l - Log ratio operator

X_m - Mean ratio operator

Where X_1 and X_2 are two multi-temporal SAR images and where μ_1 and μ_2 are local mean values of images X_1 and X_2.The changed image obtained from these ratio operators are then given to image fusion using DWT.

B. Image fusion using DWT

Image fusion may be a technique which gathers all the important information from multiple images and offers the result as one image. The obtained single image is more informative than the only source images. The utilization of image fusion isn't only to scale back the information but it provides more appropriate images for human and machine perception.

Most recent technique of image fusion is the Wavelet fusion. The wavelet technique isolates images both in space and time, so detailed information are often easily extracted from the image here than the log and mean ratio operators. In wavelet fusion images are divided to wavelet bands. L and H represents low and high frequency bands. LL denotes the approximate portion of the image, LH HL and HH denotes the horizontal, vertical and diagonal direction portions of the image.

Xm and Xl denotes the output images of mean and log ratio operators. LFB and HFB are the low and high frequency bands. LL, LH, HL, HH are the wavelets. Dwt denotes the discrete wavelet transform. Idwt is the Inverse discrete wavelet transform. Xf denotes the fused image.

The source image is that the output image of log and mean ratio operators. Both the images are converted to wavelets as LL, LH, HL and HH bands. The fusion rule is of two types i) average rule ii) max rule. The LL bands have the approximate information of the image are they're subjected to average band. LH, HH and HL bands are subjected to the max rule. These are then passed to the low and high band. The images obtained from Low Frequency and High Frequency bands are then fused to make fused wavelet coefficients. Finally, by applying IDWT the fused image is obtained. The fused image has more information of the changed region than the separate source images. Thus the kappa and Percentage of correct classification are more for the fused image compared to the source images (i.e. mean and log ratio image).Output of image fusion is given to median filter to avoid noise.

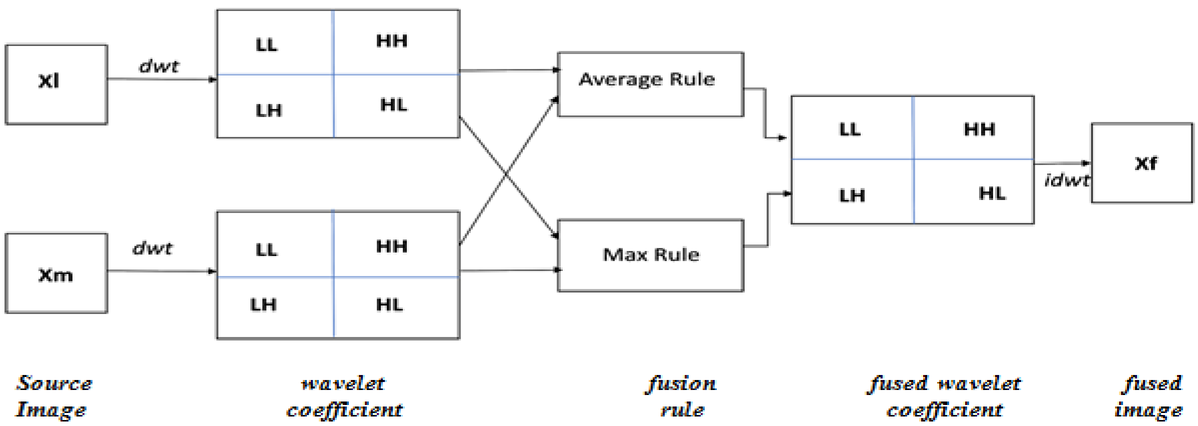

Fig 2. Discrete wavelet transform for image fusion.

C. Changed Area Detection Using RFLICM

RFLICM is a novel fuzzy clustering technique in which the local information are taken into account while computation. It replaces spatial distance as a local similarity measure and adopts local variation. In order to prove that RFLICM is more accurate than the other fuzzy techniques such as FCM and FLICM the fused image is treated with all the three techniques. The main purpose of finding the is noise sensitive and has no spatial information. FCM has been modified by incorporating spatial and local gray level difference image is to detect the changed and unchanged regions. Clustering is a process of dividing the data points into groups which are called clusters. The data points of the same group are mostly similar with the data points belonging to that group. They will be dissimilar to data points in the other group. Fuzzy C Means Clustering allows one data point to belong to two or more clusters. It is mainly used for data recognition. The main drawback of FCM algorithm is that it information. Thus they are more robust than the older one and less sensitive to noise. In the improved versions of FCM a additional parameter is applied in order to cope up with the noise and to reduce the loss of information. The selection of this parameter is not an easy task. This involves trial and error methods and experience. Taking this all into consideration Krinidis Stelios proposed a robust FCM algorithm with local gray level information and spatial context. This algorithm is the FLICM algorithm. In this the novel fuzzy factor is introduced to improve the cluster performance.

The FLICM algorithm differs from reformulated algorithm only by the fuzzy factor. The FLICM fuzzy factor can be given as

$$\mathbf{G_{K_i} = i \sum_{jeN_i} \frac{1}{p_{ij}+1} \left(1-u_{kj}\right)^m \|x_i - v_k\|^2}$$

But FLICM has the following drawbacks which can be discussed through the following 2 cases.

CASE 1

Consider a 3 x 3 window with a Centre pixel not affected by noise. An example is given in Table 1.Some pixels within the local windows are affected by noise. The difference between the center pixel and the A is more compared with that of B. In order to reduce the influence of the noisy pixel the weightings of A should be stronger than pixel B. But the damping extent of the neighbor with the spatial distance shows opposite trend.

A(120)	22	13
32	20	35
28	B(90)	27

Fig 3. Centre pixel is not noise

CASE 2

Consider a 3x3 window with the center pixel affected by noise and the other local window pixels are not affected by noise and are homogeneous. An example is given in Table 2. The difference between the other pixels and the center pixel is far different. The factor introduced here should treat the damping extent of the pixels separately but it is simply divided to only two values (0.414 and 0.5). It fails to analyze properly.

7	99	116
90	20	67
110	88	75

Fig 4. Centre pixel is affected by noise

0.414	0.5	0.414
0.5	0.5	
0.414	0.5	0.414

Fig 5. Damping extent of the neighboring pixel

To overcome the above cases slight modifications were done in the fuzzy factor and a new algorithm is proposed. This algorithm is the Reformulated Fuzzy C Means Clustering Algorithm (RFLICM).

The RFLICM algorithm can be given as:

Step 1) Set the number 'C' of the cluster prototype, the Fuzzification factor 'm' and the stopping threshold condition

Step 2) Initialize randomly the fuzzy partition matrix

Step 3) Set the loop counter value as b=0

Step 4) Calculate the cluster prototype using

$$v_k = \frac{\sum_{i=1}^{N} u_{k_i}^{m} x_i}{\sum_{i=1}^{N} u_{k_i}^{m}} \tag{6}$$

Where v is the centre of the cluster, U is the randomly initialized fuzzy partition matrix and x is the fused image. u_{k_i} is the fuzzy membership of the gray value 'i' with respect to the cluster 'k'. 'm' is the window size.

Step 5) Calculate the fuzzy partition matrix us

$$u_{k_i} = \frac{1}{\sum_{j=1}^{C} \left(\frac{\|x_i - v_k\|^2 + G'_{k_i}}{\|x_i - v_j\|^2 + G'_{j_i}} \right)^{\frac{1}{(m-1)}}} \tag{7}$$

Where $\|x_i - v_k\|^2$ is the Euclidean distance between object and the cluster center. G'_{k_i} is the novel fuzzy factor introduced to improve the clustering efficiency. The 'j'th pixel represents the neighboring pixel of the window near 'i'.

Step 6) The value of Fuzzy factor G'_{k_i} can be calculated using

If $C_u^j \geq \overline{C_u}$ then G can be given as

$$G'_{k_i} = \sum_{j\in N_i} \frac{1}{2+\min((c_u^j/c_u)^2 \cdot (c_u/c_u{}^j)^2) \times (1-u_{k_j})^m \|x_j - v_k\|^2}$$

Else

$$G'_{k_i} = \sum_{j\in N_i} \frac{1}{2-\min((c_u^j/c_u)^2 \cdot (c_u/c_u{}^j)^2) \times (1-u_{k_j})^m \|x_j - v_k\|^2}$$

The value of C can be calculated as

$$C_u = \frac{\operatorname{var}(x)}{(\bar{x})^2} \tag{8}$$

Step 5) $\{U^b - U^{b+1}\} < \varepsilon$ then stop, otherwise set b=b+1 and move to step 2

Thus from the above given algorithm with a slight change in the fuzzy factor we can get more PCC and Kappa values. This can be well proved from the following results.

D. Pixel Variation Calculation

For calculating the variation in pixel of the proposed method image with the ground truth image we have used peak signal to noise ratio. The PSNR is a measure of one's perception of the quality of the reconstruction. Although a high PSNR generally indicates high quality reconstruction, in some cases it may not. The PSNR is easily defined by the Mean Squared Error.

MSE and PSNR can be calculated using:

$$\boldsymbol{MSE = \frac{1}{mn}\sum_{i-0}^{m-1}\sum_{i-0}^{n-1}[I(i,j)-k(i,j)]^2} \tag{9}$$

$$\boldsymbol{PSR = 10.\log_{10}\left(\frac{MAX^2 I}{MSE}\right)} \tag{10}$$

MAX_I is the maximum possible pixel value of the image. I and K represent the proposed method output and ground truth image.

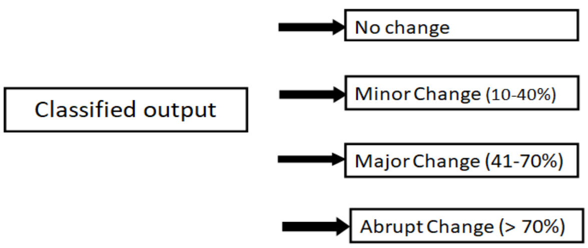

Fig 6. Classified output after pixel variation

The output of the pixel variation is classified as No change when the variation is less than 10.

The output of the pixel variation is classified as Minor change when the variation is between 10 and 40.

The output of the pixel variation is classified as Major change when the variation is between 41 and 70

The output of the pixel variation is classified as Abrupt change when the variation is greater than 70.

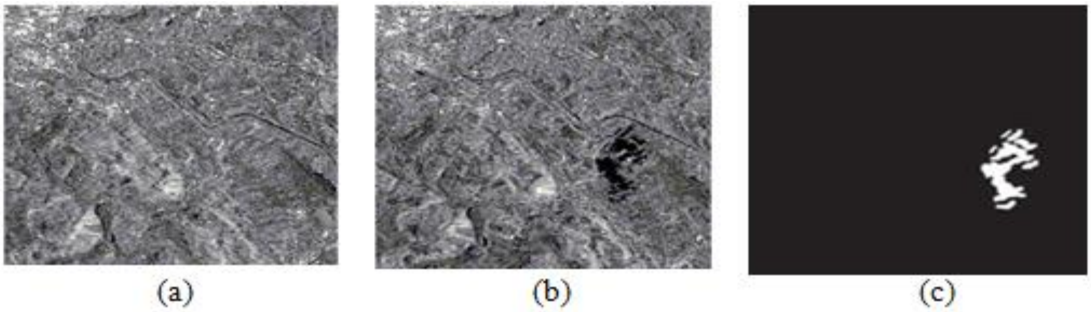

Fig 7.(a) City of Bern taken at APRIL 1999 (b) City of Bern taken at May 1999(c) Ground Truth.

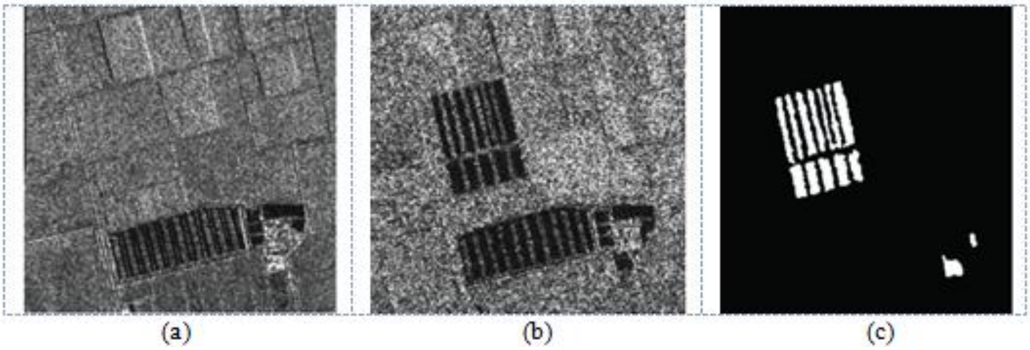

Fig 8. Yellow river estuary dataset (a) Image taken at June 2008 before planting (b) Image taken at June 2009 after planting (c) Ground truth image.

A. Result of Bern dataset

The image obtained after log, mean ratio operators and image fusion with DWT is give as follows:

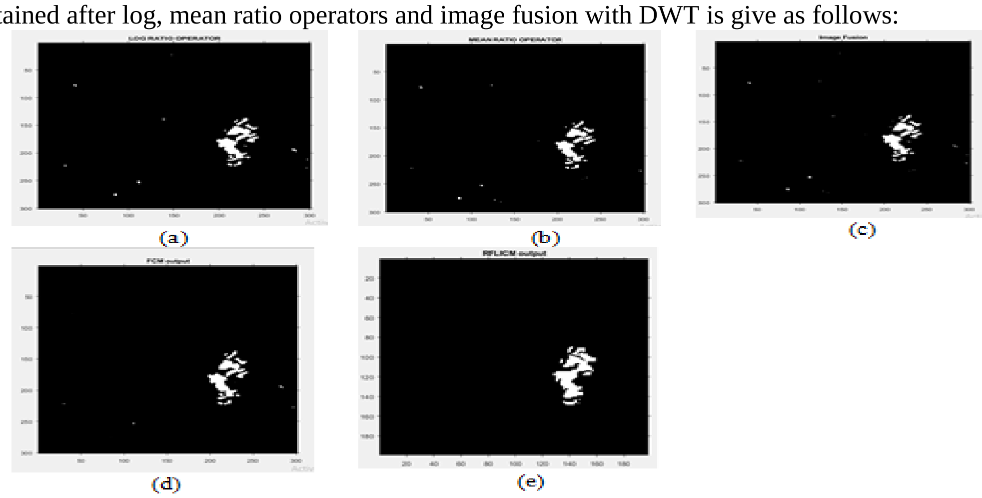

Fig 9. Result of flood images of BERN city (a) Log ratio operator; (b)Mean Ratio Operator ;(c)Image Fusion using DWT; (d) FCM; (e) Proposed.

B. Result of Yellow river estuary dataset

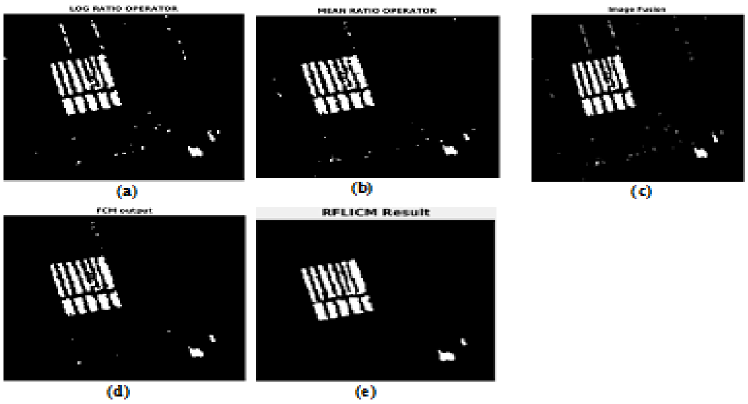

Fig 10. Result of yellow river dataset (a) Log ratio operator; (b)Mean Ratio Operator ;(c)Image Fusion using DWT; (d) FCM; (e) Proposed.

III. Results and Analysis

In order to prove the efficiency of RFLICM algorithm over other algorithms the SAR image obtained from flood area of the Bern city is taken.

The performance analysis of the images can be calculated from the two factors Percentage of correct classification (PCC) and Kappa. This can be found out from True Positive (TP), True Negative (TN), False Positive (FP), and False Negative (FN). The percentage of correct classification can be obtained from the formula:

$$PCC = (TP + TN)/ (TP = TN = FP = FN) \qquad (11)$$

TP = No of pixels detected as the changed area
TN=no of pixels detected as unchanged image
FP=unchanged pixels falsely classified as changed
FN=changed pixels that are undetected.

If the change detected image and the ground truth image are completely same then the kappa value is 1. Otherwise the kappa value will be less than 1. PCC and Kappa value should be as high as possible in order to prove the effectiveness of RFLICM over other algorithm.

C. Performance Analysis

Table 1. Change detection results of Bern flood image dataset.

OPERATORS	PPC(%)	KAPPA
LOG RATIO	98.7816	0.8483
MEAN RATIO	99.1974	0.8506
FUSION	99.4618	0.8954
FCM	99.471	0.9396
RFLICM	99.7791	0.9725

Table 2. Change detection results of Yellow river Estuary dataset.

OPERATORS	PPC	KAPPA
LOG RATIO	87.345	0.412
MEAN RATIO	87.564	0.443
FUSION	87.968	0.668
FCM	93.762	0.821
RFLICM	98.0124	0.935

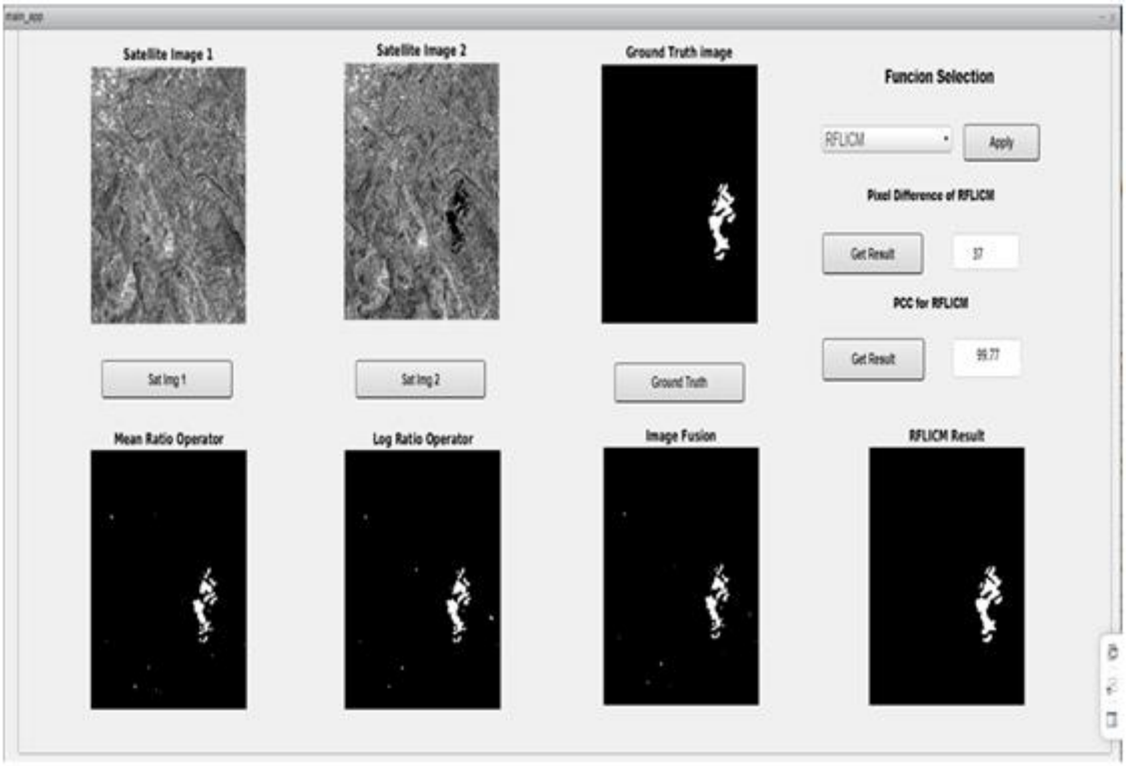

Fig 11.GUI: Bern flood image.

IEEE paper	PCC	Kappa
M. Gong, Z. Zhou and J. Ma, "Change Detection in Synthetic Aperture Radar Images based on Image Fusion and Fuzzy Clustering," in *IEEE Transactions on Image Processing*, vol. 21, no. 4, pp. 2141-2151, April 2012. [16]	99.68%	0.871
M. N. Sumaiya and R. Shantha Selva Kumari,"Unsupervised edge enhancement algorithm for SAR images using exploitation of wavelet transform coefficients," *2014* [19]	99.70%	0.8782
Proposed method	99.779%	0.9725

From the above performance analysis it can be clearly noticed that the PCC and kappa values are higher for RFLICM compared to other operators. The variation of pixels can be calculated by comparing the change detected image with the ground truth image. The variation of pixels from the above analysis is lesser for RFLICM than other techniques. Thus it can be said clearly that RFLICM has more accuracy in change detection compared to FCM. The pixel variation of Bern flood image has a lesser value of 37%which denotes minor change. The pixel variation of yellow river estuary is calculated as 22% a minor chang**e.**

D. Performance comparison

To prove the efficiency of our paper with other papers we have made a comparison table for PCC and Kappa performance of Bern flood area SAR image dataset.

Thus from the above comparison table it is clear that the techniques and flow of our paper is more accurate.

IV. Conclusion

In this paper, we have presented a novel SAR image change detection technique using RFLICM. The original SAR images are subjected to different operators' log, mean, image fusion, FCM and RFLICM. The log ratio operator is used to produce the difference image with enhanced low intensity pixels. The mean ratio operator suppresses the unchanged region and improves the homogeneity of the changed region. Image fusion technique is mainly used to restore the background information. By analysing with various parameters such as TP, TN, FP, FN, PCC, Kappa, pixel variation it is clearly noticed that RFLICM has high values of PCC and Kappa values compared to other techniques.

From the result it is also seen that RFLICM has less spots compared to other techniques. Thus RFLICM has high accuracy compared to other techniques.

References

1. S.Marchesi, F. Bovolo, and L. Bruzzone, “A context-sensitive technique robust to registration noise for change detection in VHR multispectral images,” IEEE Trans. Image Process., vol. 19, no. 7, pp. 1877–1889, Jul. 2010.

2. A. Robin, L. Moisan, and S. Le Hegarat-Mascle, “An a-contrario approach for subpixel change detection in satellite imagery,” IEEE Trans. Pattern Anal. Mach. Intell., vol. 32, no. 11, pp. 1977–1993, Nov. 2010.

3. S. S. Ho and H. Wechsler, “A martingale framework for detecting changes in data streams by testing exchangeability,” IEEE Trans. Pattern Anal. Mach. Intell., vol. 32, no. 12, pp. 2113–2127, Dec. 2010.

4.S. Krinidis and V. Chatzis, “A robust fuzzy local information C-means clustering algorithm,” IEEE Trans. Image Process., vol. 19, no. 5, pp. 1328–1337, May 2010.

5.W. Yang, X. Yang, T. Yan, H. Song, and G.-S.Xia, "Region-based change detection for polarimetric SAR images using Wishart mixture models," IEEE Transactions on Geoscienceand Remote Sensing, vol. 54, pp. 6746-6756, 2016.

6. Y. Zheng, L. Jiao, H. Liu, X. Zhang, B. Hou, and S. Wang, "Unsupervised saliency-guided SAR image change detection," Pattern Recognition, vol. 61, pp. 309-326, 2017.

7. L. Hu, C. Qi, S. Chen, and Q. Wang, "An Improved Heuristic Optimization Algorithm for Feature Learning Based on Morphological Filtering and Its Application," IEEE Access, vol. PP, pp. 1-1, 2018.

8. F. G. B. D.Natale and G. Boato, "Detecting Morphological Filtering of Binary Images," IEEE Transactions on InformationForensics & Security, vol. 12, pp. 1207-1217, 2017.

9. V. T. Vu, N. R. Gomes, M. I. Pettersson, P. Dammert, and H. Hellsten, "Bivariate Gamma Distribution for Wavelength-Resolution SAR Change Detection," IEEETransactions onGeoscience and Remote Sensing, pp. 1-9, 2018.

10.M. Jia and L. Wang, "Novel class-relativity non-local means with principal component analysis for multitemporal SAR image change detection," International Journal of Remote Sensing, vol. 39, pp. 1068-1091, 2018

11. Shang R., Qi L., Jiao L., Stolkin R., Li Y. Change detection in SAR images by artificial immune multi-objective clustering. Eng. Appl. ArtifIntell. 2014; 31: 53–67. doi: 10.1016/j.engappai.2014.02.004.

12. Simard M., Degrandi G., Thomson K.P.B., Benie G.B. Analysis of speckle noise contribution on wavelet decomposition of SAR images. IEEE Trans. Geosci. Remote Sens. 2002; 36: 1953–1962. doi: 10.1109/36.729367.

13.Chen J., Kang X., Liu Y., Wang Z.J. Median Filtering Forensics Based on Convolutional Neural Networks. IEEE Signal Process. Lett. 2015; 22: 1849–1853.
doi: 10.1109/LSP.2015.2438008.

14.Ikuta C., Zhang S., Uwate Y., Yang G., Nishio Y.A novel fusion algorithm for visible and infrared image using non-subsampled contourlet transform and pulse-coupled neural network; Proceedings of the International Conference on Computer Vision Theory and Applications; Lisbon, Portugal. 5–8 January 2015; pp. 160–164.

15.Paul, Lincy and P. Ramamoorthy. “Synthetic Aperture Radar Image Change Detection Using Fuzzy C-Means Clustering Algorithm.” (2013).

16.M. Gong, Z. Zhou and J. Ma, "Change Detection in Synthetic Aperture Radar Images based on Image Fusion and Fuzzy Clustering," in IEEE Transactions on Image Processing, vol. 21, no. 4, pp. 2141-2151, April 2012.

17.M. N. Sumaiya and R. Shantha Selva Kumari, "Logarithmic Mean-Based Thresholding for SAR Image Change Detection," in IEEE Geoscience and Remote Sensing Letters, vol. 13, no. 11, pp. 1726-1728, Nov. 2016.

18.Sumaiya , M. and Shantha Selva Kumari, R.., 2017. Gabor filter based change detection in SAR images by KI thresholding. Optik , 130 , pp.114-122.

19.M. N. Sumaiya and R. Shantha Selva Kumari, "Unsupervised edge enhancement algorithm for SAR images using exploitation of wavelet transform coefficients," 2014 International Conference on Communication and Network Technologies, Sivakasi, 2014, pp. 57-61, doi: 10.1109/CNT.2014.7062725.

20.C. Mu, Chengzhou Li, Y. Liu, Menghua Sun, Licheng Jiao and R. Qu, "Change detection in SAR images based on the salient map guidance and an accelerated genetic algorithm," 2017 IEEE Congress on Evolutionary Computation (CEC), San Sebastian, 2017, pp. 1150-1157.
doi: 10.1109/CEC.2017.7969436.